Cell Stem Cell
Article

Generation of Multipotent Lung and Airway Progenitors from Mouse ESCs and Patient-Specific Cystic Fibrosis iPSCs

Hongmei Mou,[1,2] Rui Zhao,[1,2] Richard Sherwood,[5] Tim Ahfeldt,[1,6] Allen Lapey,[3] John Wain,[1,4] Leonard Sicilian,[2] Konstantin Izvolsky,[1] Frank H. Lau,[4] Kiran Musunuru,[1,5,6,7] Chad Cowan,[1,6,7] and Jayaraj Rajagopal[1,2,3,7,*]
[1]Center for Regenerative Medicine
[2]Department of Internal Medicine, Pulmonary and Critical Care Unit
[3]Department of Pediatrics, Pulmonary Unit
[4]Department of Surgery
Massachusetts General Hospital, Boston, MA 02114, USA
[5]Department of Medicine, Brigham and Women's Hospital, 77 Avenue Louis Pasteur, Boston, MA 02115, USA
[6]Department of Stem Cell and Regenerative Biology, Harvard University, 7 Divinity Avenue, Cambridge, MA 02138, USA
[7]Harvard Stem Cell Institute, Holyoke Center, 1350 Massachusetts Avenue, Cambridge, MA 02138, USA
*Correspondence: jrajagopal@partners.org
DOI 10.1016/j.stem.2012.01.018

SUMMARY

Deriving lung progenitors from patient-specific pluripotent cells is a key step in producing differentiated lung epithelium for disease modeling and transplantation. By mimicking the signaling events that occur during mouse lung development, we generated murine lung progenitors in a series of discrete steps. Definitive endoderm derived from mouse embryonic stem cells (ESCs) was converted into foregut endoderm, then into replicating Nkx2.1+ lung endoderm, and finally into multipotent embryonic lung progenitor and airway progenitor cells. We demonstrated that precisely-timed BMP, FGF, and WNT signaling are required for NKX2.1 induction. Mouse ESC-derived Nkx2.1+ progenitor cells formed respiratory epithelium (tracheospheres) when transplanted subcutaneously into mice. We then adapted this strategy to produce disease-specific lung progenitor cells from human Cystic Fibrosis induced pluripotent stem cells (iPSCs), creating a platform for dissecting human lung disease. These disease-specific human lung progenitors formed respiratory epithelium when subcutaneously engrafted into immunodeficient mice.

INTRODUCTION

The discovery of embryonic stem cells (ESCs) and induced pluripotent stem cells (iPSCs) has resulted in an unprecedented opportunity to produce tissue-specific cell types that can be used in human disease modeling, drug screening, and patient-specific therapies. Generating disease-specific lung epithelial cells from human lung disease-specific iPSCs is particularly important because murine models of lung disease often do not phenocopy human lung disease. A prime example of the failure of mouse models to mimic human disease is the *Cftr* knockout mouse that does not display the Cystic Fibrosis (CF) disease-associated lung pathology observed in human patients (Snouwaert et al., 1992; Clarke et al., 1992; Guilbault et al., 2007). Extraordinary experiments have created new animal models of CF in both the ferret and the pig nearly 2 decades after the CFTR gene was cloned (Rogers et al., 2008; Stoltz et al., 2010; Sun et al., 2010; Kerem et al., 1989; Riordan et al., 1989). These heroic experiments allow the modeling of CF at a whole-animal level.

The work presented herein is an attempt to add a human model system to these remarkable prior efforts. Although it does not permit the analysis of the disease in the full animal context, the iPSC system will allow patient specificity. It is known that many patients with the same CFTR mutations do not have a similar clinical course (Kerem et al., 1990, 1992; Cutting, 2005). Some of this variability is thought to result from disease-modifying genes (Drumm et al., 2005; Haston and Hudson, 2005; Knowles, 2006). Using patient-specific iPSCs from patients such as these will permit the study of CF clinical variability in the laboratory without the need to identify these genes beforehand. Building on the remarkable recent success of the first drug to target the CFTR channel defect directly in patients with the rare G551D mutation (Accurso et al., 2010), it is clear how this iPSC-based system could serve as a platform for finding therapeutics for every patient with CF.

Although many iPSCs from patients with lung diseases are currently being produced, the major obstacle preventing the actual development of human lung disease models using these cells is the inability to convert them into lung progenitors and subsequently into differentiated pulmonary epithelial cell types. Several attempts to produce pulmonary epithelial cells from mouse and human ESCs have been made. Most investigators have focused on the generation of type II pneumocytes (Van Vranken et al., 2005; Samadikuchaksaraei et al., 2006; Wang et al., 2007). Fewer studies have targeted the differentiation of airway epithelial cells from pluripotent stem cells despite the fact that airway diseases such as asthma, CF, bronchitis, and bronchogenic carcinoma are, in aggregate, more prevalent than the diseases of the alveoli such as emphysema.

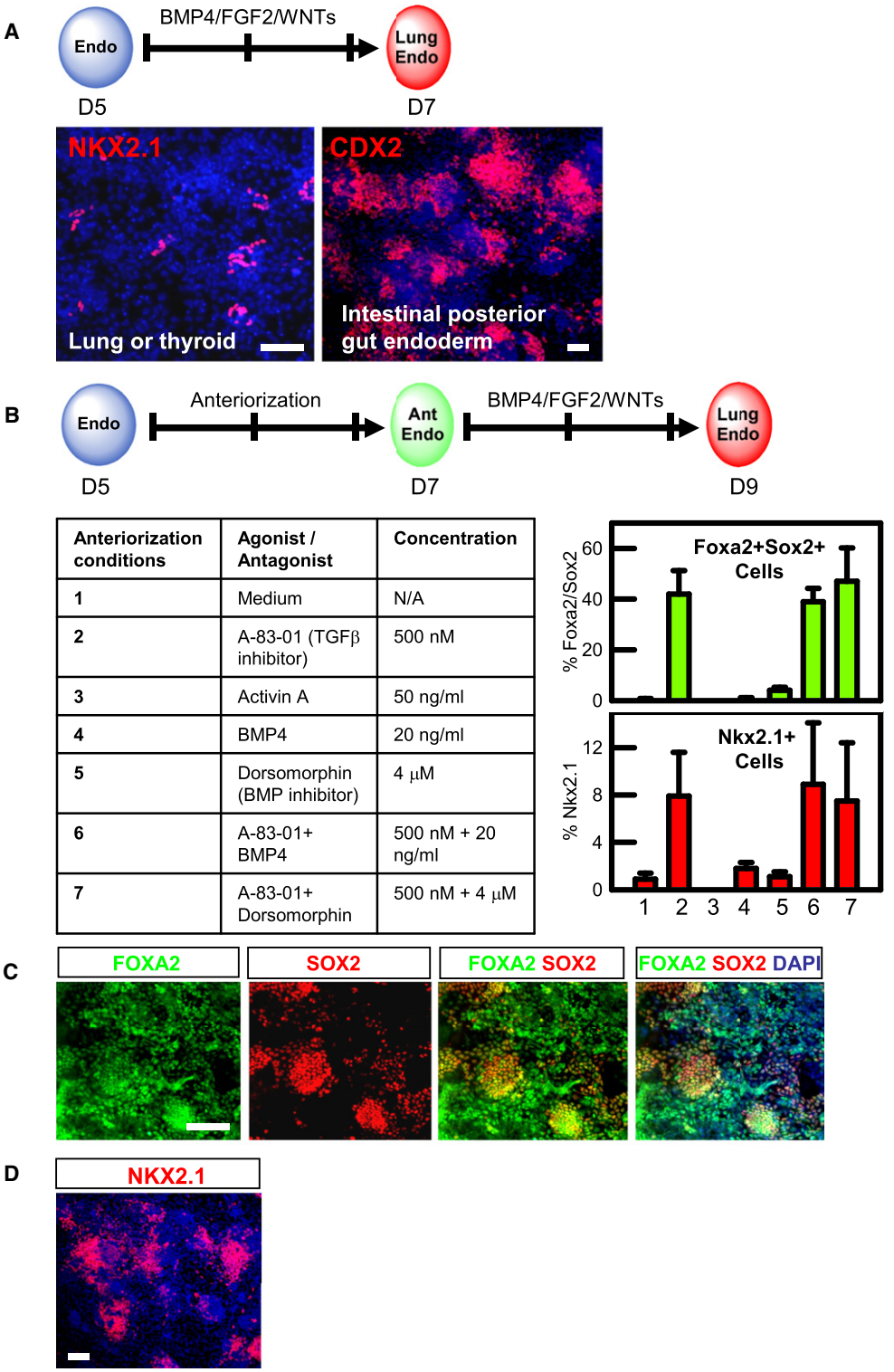

Anteriorization conditions	Agonist / Antagonist	Concentration
1	Medium	N/A
2	A-83-01 (TGFβ inhibitor)	500 nM
3	Activin A	50 ng/ml
4	BMP4	20 ng/ml
5	Dorsomorphin (BMP inhibitor)	4 μM
6	A-83-01+ BMP4	500 nM + 20 ng/ml
7	A-83-01+ Dorsomorphin	500 nM + 4 μM

Figure 1. Anteriorization of Endoderm to Foregut Endoderm Promotes Nkx2.1+ Cell Differentiation

(A) Administration of 20 ng/ml BMP4, 20 ng/ml FGF2, and 5 nM GSK3iXV to definitive endoderm resulted in hindgut differentiation with CDX2 expression, and minimal NKX2.1 induction. Scale bar, 50 μm.

(B) Definitive endoderm was treated with different combinations of BMP4/TGFβ agonists and antagonists as listed in the table for 2 days. The Foxa2+/Sox2+ cells were quantified as a percentage of positive cells out of the total number of Foxa2+ cells. The cells were further treated with 20 ng/ml BMP4, 20 ng/ml FGF2, and 5 nM GSK3iXV to induce NKX2.1 expression. The percentage of Nkx2.1+ cells was quantified as a percentage of the total cells present. All data were averaged from three independent experiments.

Prior attempts (Coraux et al., 2005; Van Haute et al., 2009) to generate functional pulmonary epithelium from ESCs were characterized by the stochastic production of limited numbers of cells and the generation of mixed cell populations, which contain undifferentiated pluripotent stem cells that carry a significant risk of teratoma formation after transplantation. Others have utilized incompletely defined media to induce respiratory cell differentiation (such as exposure of human ESCs to tumor cell extract; Roszell et al., 2009) or have used genetically modified pluripotent stem cells that were selected based upon the presence of a drug resistance gene (Wang et al., 2007). Unfortunately, genetic modulation raises the possibility of the introduction of deleterious mutations in the resulting cells.

Our overall strategy is to employ a stepwise differentiation approach that mimics the timing and coordination of the signaling pathways that guide lung development. Since there is limited data concerning the embryonic signaling pathways that regulate human lung organogenesis, we hypothesized that human lung organogenesis is, in part, analogous to mouse organogenesis. Therefore, knowledge of mouse lung development can serve as a roadmap to guide human iPSC differentiation strategies. Mechanisms that regulate mouse embryonic endoderm regionalization, lung specification, and subsequent progenitor patterning and growth have been well studied (reviewed in Morrisey and Hogan, 2010). The onset of lung specification within the endoderm is accompanied by *Nkx2.1* expression and the downregulation of *Sox2* along the dorsal-ventral axis of the gut tube (Lazzaro et al., 1991; Minoo et al., 1999; Que et al., 2009). Later, *Sox2* expression again increases in the area of the future trachea, bronchus, and bronchioles. The Nkx2.1+Sox2+ cells in this region of the embryonic lung are airway progenitor cells that give rise to the mature airway epithelium (Que et al., 2009). In contrast, *Sox9*, *FoxP2*, and *ID2* are expressed in the distal embryonic lung bud tip and mark a multipotent embryonic lung progenitor population (Perl et al., 2005; Shu et al., 2007; Rawlins et al., 2009) capable of producing all of the cell types of the airway and alveoli. We report the differentiation of these two early progenitor cell populations from mouse and human pluripotent stem cells.

Because Nkx2.1 is the earliest marker of lung endoderm distinguishing it from the rest of the foregut endoderm, we have focused on producing Nkx2.1+ lung endoderm that is devoid of Nkx2.1+ thyroid endoderm and neuronal progenitors. A recent report using human ESCs demonstrated that a differentiation strategy based on mimicking mouse gut organogenesis led to the production of anterior foregut cells and Nkx2.1+ cells with efficiencies up to 30% (Green et al., 2011). However, these Nkx2.1+ cells were not demonstrated to be composed of purely lung progenitors. TUJ1 (a marker of neuronal tissue) and PAX8 (a marker of thyroid tissue) expression was not evaluated at the single-cell level by antibody costaining with an Nkx2.1 antibody. Development of a novel strategy to produce Nkx2.1+ progenitors that reflect only lung and not thyroid or brain differentiation is therefore needed (Watanabe et al., 2005), and the technique must be applicable to human disease-specific iPSCs in order for the technique to become widely relevant to the study of human lung disease.

Building on the aforementioned studies, we report an efficient and consistent step-wise differentiation method to generate definitive endoderm (DE), foregut endoderm, early lung endoderm, multipotent Nkx2.1+ embryonic lung progenitor cells, and airway progenitor cells beginning with mouse ESCs and subsequently with lung disease-specific human iPSCs. We show that a high dose of Activin, transient WNT activation, and staged BMP4 inhibition converts ESCs into DE with high efficiencies. Further inhibition of TGFβ alone is sufficient to "anteriorize" endoderm into Sox2+ foregut endoderm. We show that this anteriorization of the endoderm to foregut endoderm enhances the ultimate differentiation of Nkx2.1+ cells at later steps of the strategy. BMP4, FGF2, and WNT are each necessary for induction of the Nkx2.1+ immature lung progenitors. These early progenitors can mature into Nkx2.1+Sox2+ proximal progenitor cells and Nkx2.1+p63+ airway basal stem cells in vitro, and can differentiate into airway epithelium. A modification of this strategy was used to produce human disease-specific immature airway epithelium derived from CF iPSCs, creating a new platform for dissecting human lung disease.

RESULTS

Stage-Specific TGFβ Inhibition Regionalizes Naive Endoderm to Anterior Foregut Endoderm and Facilitates the Differentiation of Nkx2.1+ Cells

A recent report described a monolayer-based strategy using synergistic activation of Nodal and Wnt-β-catenin signaling as well as staged BMP4 inhibition to direct mouse ESCs toward an endoderm fate with high efficiency (Sherwood et al., 2011). Here, we adapted this technology to generate DE from mouse ESCs (Figure S1A available online). This protocol resulted in a remarkable 80%–90% of cells being converted into DE based on the dual expression of the endoderm transcription factors FOXA2 and SOX17 (Figure S1B). Next, we asked if the newly generated DE cells have the competence to generate Nkx2.1+ cells. After culturing them for 2 days in serum-free medium containing BMP4, FGF2, and GSK3iXV (a WNT agonist) (Figure 1A), we observed that less than 1% of the cells were Nkx2.1+ (Figure 1A). However, more than 60% of the cells were Cdx2+, suggesting that the majority of the cells were specified to a hindgut fate (Figure 1A). Because the endoderm cells at this stage did not efficiently differentiate into Nkx2.1+ cells, we sought to test if an "anteriorization" step would facilitate lung fate specification. Snoeck and colleagues reported that Noggin (BMP inhibitor) synergized with SB431542 (a TGFβ inhibitor) to suppress a posterior endoderm fate (Cdx2+) in favor of an anterior endoderm fate (Sox2+) (Green et al., 2011). Because we had already incorporated BMP inhibition during DE generation (Figure S1A), we asked whether continuous BMP inhibition is necessary for

(C) Representative immunofluorescence staining showing Foxa2+ and Sox2+ double positive cells after 2 days of treatment with 500 nM A-83-01. Scale bar, 100 μm.

(D) Representative immunofluorescence staining showing NKX2.1 induction from A-83-01 treated endoderm cells after BMP4/FGF2/GSK3iXV treatment for 2 days. Scale bar, 100 μm.

anteriorization or if TGFβ inhibition alone was sufficient for anterior patterning. Hence, we treated endoderm with combinations of Activin (TGFβ agonist), A-83-01 (TGFβ antagonist), BMP4, and Dorsomorphin (BMP4 antagonist) for 2 days (Figure 1B). We then compared the number of FoxA2+Sox2+ anterior endoderm cells to the total number of FoxA2+ endoderm cells (Figure 1B). We also exposed the treated cells to the BMP4/FGF2/WNT agonist cocktail for another 2 days to examine their competence to generate Nkx2.1+ cells (Figure 1B). Our results revealed that TGFβ inhibition itself was sufficient to increase FoxA2+Sox2+ anterior endoderm (40%–55%, compared to <0.1% in medium alone; Figures 1B and 1C) and enhance the competence of endoderm cells to form Nkx2.1+ cells (~7%–13% as compared to <1% without regionalization; Figures 1B and 1D). We observed that continuous Activin treatment resulted in rare FoxA2+Sox2+ cells and few Nkx2.1+ cells (Figure 1B), suggesting that the optimal duration of Activin exposure was important. We also found that additional BMP4 inhibition was not required for the generation of FoxA2+Sox2+ cells and ultimately may result in slightly lower percentages of Nkx2.1+ cells (Figure 1B). We also observed less neuroectodermal marker TUJ1 if BMP4 was present between days 5 to 7 (data not shown), in agreement with the finding that BMP4 suppresses neuronal commitment and promotes nonneural lineage differentiation from ESCs (Zhang et al., 2010). FGF and WNT signaling have been shown to maintain hindgut identity and actively repress foregut endoderm differentiation (Wells and Melton, 2000; Ameri et al., 2010). Therefore, we also tested if their inhibition would enhance anteriorization together with a TGFβ inhibitor. Subsequent experiments revealed that an FGF antagonist (PD173074) induced cell death, while a WNT antagonist (IWR-1) did not increase the FoxA2+Sox2+ population (data not shown).

Mouse ESC-Derived Nkx2.1+ Cells Are Devoid of Neuronal and Thyroid Markers, Are Proliferative, and Contain Distal Multipotent Lung Progenitors and Proximal Airway Progenitors

Nkx2.1 is not a specific marker of the lung, and its expression is also found in the thyroid and ventral forebrain (Figure S2A). Therefore, it was important to determine the identity of the Nkx2.1+ cells generated in our culture system. Unfortunately, there are no reliable markers of the lung lineage at embryonic stage E9 that are not expressed in the brain or thyroid. Surfactant protein C (Sp-C), which is the most specific marker for lung epithelial progenitors, is not detected until E10–E11 (Wert et al., 1993). SOX9 and FOXP2 are indeed coexpressed with NKX2.1 in distal lung multipotent epithelial progenitor cells (Figure S3B) and are not found in brain or newly specified thyroid (Figure S2B and data not shown), but their expression is not evident until after E11–E12. SOX2, on the other hand, is expressed in the E9 lung endoderm (Figure S2A) and later in airway epithelial progenitors (Figures S3A and S3B), but SOX2 can also be found in NKX2.1-expressing cells in ventral forebrain (Figures S2A and S2C). Thus, at the earliest stage of lung endoderm specification (E8.75–E9), none of these markers (SPC, SOX2, SOX9, or FOXP2) can be used to reliably and uniquely identify lung cells. In contrast, TUJ1 expression in Nkx2.1+ cells in ventral forebrain begins at E8.0 and continues to be present thereafter in ventral forebrain and not in thyroid or lung (Figures S2B and 2C), making *Tuj1* expression a specific indicator of neuronal cell identity within the NKX2.1 domain. PAX8 expression is detected in the primordial thyroid at E8.75 at the time of thyroid specification (Figure S2B), but not in the lung or brain. Therefore, PAX8 can be used as a specific indicator of thyroid cell identity in the NKX2.1 domain (Figures S2B and S2C). In summary, we conclude that at the early specification stage, we can regard Nkx2.1+/Tuj1–/Pax8– cells as likely to be of lung cell lineage. Accordingly, we interrogated our ESC-derived Nkx2.1+ cells for TUJ1 and PAX8 expression to exclude neuronal and thyroid identity (Figure 2A). As expected for any Nkx2.1+ cell in the embryo (thyroid, lung, and ventral forebrain), all of our ex vivo differentiated Nkx2.1+ cells costained with FOXA2 (Figure 2A). We detected a small subset of Tuj1+ cells in the cultures, but these neuronal cells did not overlap with the Nkx2.1+ cells (Figure 2A). We did not detect any Pax8+ cells in our culture (Figure 2A; Figure S2B and data not shown). Therefore, this suggests that the Nkx2.1+ cells that we differentiate in vitro represent lung endoderm cells. These Nkx2.1+ cells are proliferative, with more than half expressing Ki67 (Figure 2B).

In the mouse, *Sox2* is rapidly downregulated in the foregut prelung endoderm just as *Nkx2.1* expression initiates in this same prelung endoderm during the process of lung specification at E9 (Figure S3A). Thus the very earliest lung endoderm cells are Nkx2.1+ and Sox2-low cells. Soon thereafter, sustained high-level SOX2 expression is detected in the proximal airway epithelial progenitors of the future trachea, bronchus, and bronchioles during the process of branching morphogenesis (Figures S3A and S3B). Airway progenitors are therefore Nkx2.1+Sox2+. In contrast, SOX9 and FOXP2 are expressed exclusively in the distal tip multipotent lung progenitor cells (Figure S3B), making SOX9 and FOXP2 markers that uniquely identify a distinct population of multipotent embryonic lung progenitor cells within the NKX2.1 domain because they are not present in the proximal airway progenitors or the thyroid or brain as mentioned above. Therefore, we checked if our ESC-derived Nkx2.1+ cells at day 9 contained both proximal airway (Nkx2.1+Sox2+) and distal multipotent (Nkx2.1+Sox9+; or Nkx2.1+FoxP2+) progenitor cells. We counted the Nkx2.1+ cells generated from 10 independent experiments. The average proportion of airway progenitor cells (Nkx2.1+Sox2+) was 1.8% ± 0.8% out of the total Nkx2.1+ cells, while the proportions of distal multipotent progenitor cells, Nkx2.1+Sox9+ or Nkx2.1+FoxP2+, were 4.8% ± 2.5% and 6.6% ± 3.1% out of total Nkx2.1+ cells, respectively. The remaining Nkx2.1+ cells (not thyroid or neuron are cells with minimal SOX2 expression and may reflect early prelung endoderm. Thus, the majority of Nkx2.1+ cells at day 9 likely represent an early lung endoderm that has not been specified to an airway progenitor or a distal tip multipotent lung progenitor population. Figure 2C shows representative fields of cells enriched in Nkx2.1+Sox2+, Nkx2.1+Sox9+, and Nkx2.1+FoxP2+ cells. In aggregate, these results imply that ESC-derived Nkx2.1+ cells at day 9 were immature, with most lacking proximal and distal progenitor cell markers, likely representing early lung endoderm cells. Although rare, the existence of Nkx2.1+Sox2+, Nkx2.1+Sox9+, and Nkx2.1+FoxP2+ cells suggested that the ESC-derived Nkx2.1+ lung endoderm cells were differentiating

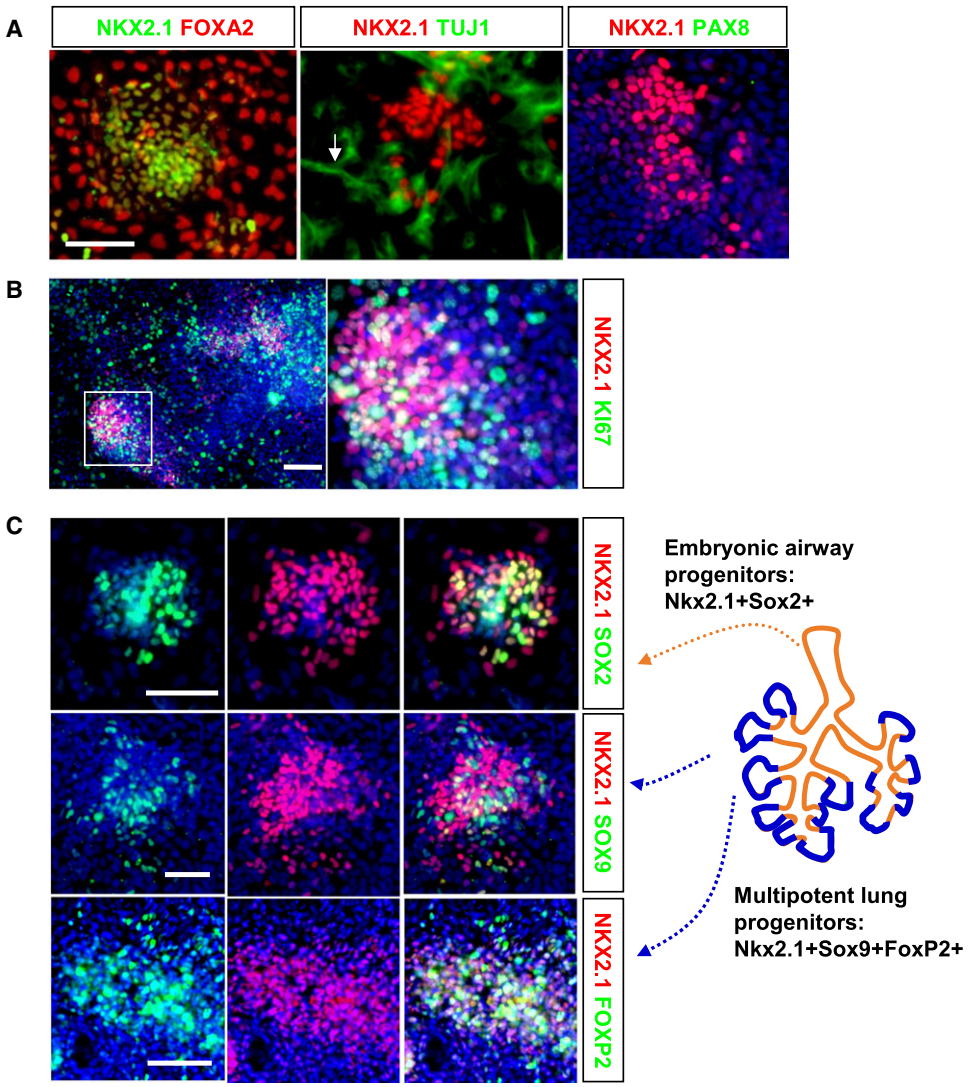

Figure 2. ESC-Derived Nkx2.1+ Cells Are Devoid of Neuronal and Thyroid Markers, Are Proliferative, and Possess Markers of Proximal and Distal Lung Endoderm

(A) Immunofluorescence staining for FOXA2, TUJ1, and PAX8 showing that Nkx2.1+ cells are positive for endodermal marker FOXA2, negative for neuroectodermal marker TUJ1 (white arrow), and negative for thyroid marker PAX8. Scale bar, 50 μm.

(B) Nkx2.1+ cells were proliferative as demonstrated by costaining for KI67. Scale bar, 100 μm.

(C) Representative immunofluorescence staining showing subpopulations of Nkx2.1+ cells are positive for SOX2 (an airway progenitor marker) and FOXP2/SOX9 (multipotent lung progenitor marker). Scale bar, 100 μm.

into progenitor cells of the airway and multipotent lung progenitor cells that could later be differentiated into mature epithelial cells.

The expression of lung and other anterior cell fate lineage genes including *FoxN1* (thymus), *Pax8* (thyroid), and *Pax9* and *Tbx1* (pharyngeal pouch endoderm) was analyzed by real-time qPCR (Figure S4A). As expected, the results showed that *Sox2* was downregulated as pluripotent cells differentiated into DE. Later, *Sox2* levels increased in accord with the expectation that anterior endoderm expresses *Sox2*. *Nkx2.1*, *Sox9*, and *FoxP2* expression was minimal in ESCs, DE, and anteriorized endoderm, but was greatly increased (10–20 fold) after stimulation with the FGF2/WNT/BMP4 induction cocktail, consistent with previous results demonstrating these lung-specific marker combinations by antibody staining (Figure 2C). Similarly, *FoxN1*, *Tbx1*, *Pax8*, and *Pax9* expression was low in ESCs, DE and anteriorized endoderm. However, in growth-factor-induced anterior foregut cells, we observed a modest increase in *Pax9* and *Tbx1* expression, whereas *FoxN1* and *Pax8* expression was still very minimal. Despite the increase in *Pax9* and *Tbx1* gene expression, we did not detect any reproducible staining for these proteins by immunofluorescence (data not shown). All of these results are consistent with our finding that a combination of FGF, BMP4, and WNT signaling predominantly drives the differentiation of lung-specific Nkx2.1+ progenitor cells from anterior endoderm.

A

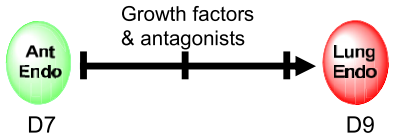

B

	Growth factors & antagonists	Concentrations
1	Medium	N/A
2	BMP4	10 ng/ml
3	BMP4	20 ng/ml
4	BMP4	100 ng/ml
5	BMP4 + Dorsomorphin	10 ng/ml + 5 μM
6	BMP4 + PD98059	10 ng/ml + 1 μM
7	FGF2	20 ng/ml
8	FGF2	100 ng/ml
9	BMP4 + FGF2	10 ng/ml + 20 ng/ml
10	BMP4 + FGF2	10 ng/ml + 100 ng/ml
11	BMP4 + FGF2 + PD173074	10 ng/ml + 20 ng/ml + 1 μM
12	BMP4 + GSK3iXV	10 ng/ml + 10 nM
13	BMP4 + GSK3iXV	10 ng/ml + 500 nM
14	BMP4 + IWR-1	10 ng/ml + 1 μM
15	BMP4 + FGF2+ GSk3iXV	10 ng/ml + 20 ng/ml + 10 nM
16	BMP4 + FGF2 + GSK3iXV	20 ng/ml + 100 ng/ml + 10 nM

C

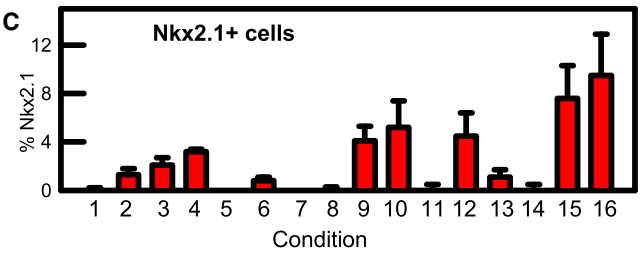

Figure 3. BMP4, FGF2, and WNT Signaling Are Necessary for Lung Specification from Foregut Endoderm Cells

(A) Schematic strategy and time frame to generate Nkx2.1+ cells from foregut endoderm cells.

(B) NKX2.1 induction using various combinations of BMP4, FGF2, WNT, and their antagonists.

(C) NKX2.1 percentage was scored as the number of Nkx2.1+ cells out of the total cell number, average of three independent experiments.

BMP4, FGF, and WNT Signaling Are Each Necessary for NKX2.1 Induction In Vitro, Recapitulating Murine Lung Development

Based on mouse genetic studies, BMP4, FGF2, and WNT signaling are each required to specify lung endoderm from the anterior foregut (Domyan et al., 2011; Goss et al., 2009; Serls et al., 2005). Therefore, we tested if we could recapitulate these findings in our in vitro mouse ESC differentiation system. To do this, we exposed the anteriorized endoderm cells to combinations of BMP4, FGF2, and WNT agonists and antagonists (Figures 3A and 3B). We found that BMP4 alone could induce NKX2.1 expression. In contrast, FGF2 or/and GSKiXV without BMP4 was not sufficient for NKX2.1 induction, suggesting that BMP4 signaling is required for lung specification (Figures 3B and 3C). Interestingly, in the presence of FGF and WNT antagonists, BMP4 could no longer induce Nkx2.1+ cells. This result implies an endogenous secretion of FGF and WNT ligands. It also suggests that FGF and WNT activation are needed for BMP4-dependent NKX2.1 specification (Figures 3B and 3C). Despite presumptive endogenous FGF signaling, an increase in FGF2 concentration upregulated Nkx2.1+ cell percentage, which is in agreement with the finding that high doses of FGF2 promote lung fate from foregut (Figures 3B and 3C; Serls et al., 2005). Compared to FGF2 signaling, exaggerated WNT activation was detrimental, with a decrease in Nkx2.1+ cells (Figures 3B and 3C) and an increase in hindgut Cdx2+ cells (data not shown), consistent with the fact that WNT signaling is known to posteriorize gut to hindgut prior to its effect on the lung (Sherwood et al., 2011).

BMP2, BMP4, and BMP7 are by far the most studied members of the BMP family. Both BMP2 and BMP4 signal through the type I receptor (ALK3), whereas BMP7 binds to a separate type I receptor (ALK2) (reviewed by von Bubnoff and Cho, 2001; Chen et al., 2004; Sieber et al., 2009; Miyazono et al., 2010). We compared the effects of BMP2 and BMP7 to BMP4 on induction of Nkx2.1+ cells from the anterior endoderm. Our results showed that BMP2 was less efficient than BMP4 at inducing Nkx2.1+ cells, while BMP7 (10 ng/ml) had no effect (Figure 4A). Even with an increased concentration (>100 ng/ml), BMP7 still failed to generate Nkx2.1+ cells (data not shown). This suggests that BMP7 signaling via the ALK2 receptor is not required for NKX2.1 induction. In canonical BMP2/4 signaling, BMP2/4 binds to BMP receptor I/II complex, leading to phosphorylation of Smad1/5/8, followed by formation of heteromeric complexes with Smad4. These complexes translocate to the nucleus and activate expression of target genes (von Bubnoff and Cho, 2001; Chen et al., 2004; Sieber et al., 2009; Miyazono et al., 2010). Besides Smad1/5/8-mediated transcription, BMP-induced receptor complexes can activate the mitogen-activated protein kinase (MAPK) pathway via ERK, JNK, or p38 (Kozawa et al., 2002). Using Dorsomorphin (a pSmad1/5/8 inhibitor) and PD98059 (a MAPKK/ERK inhibitor), we observed that Dorsomorphin completely abrogated generation of Nkx2.1+ cells, while PD98059 only partially decreased the Nkx2.1+ cell proportion (Figure 4A). We also observed significant cell death in the presence of PD98059, so we could not exclude the possibility that the decrease in Nkx2.1+ cells was due to apoptosis. In addition, Smad and MAPK-mediated pathways can be integrated (Aubin et al., 2004), and the decrease in Nkx2.1+ cells in the presence of PD98059 might also be due to a downregulation of Smad-dependent signaling. Overall, we conclude that Smad-dependent BMP2/4 signaling cascade is necessary for NKX2.1 specification from foregut cells (Figure 4B).

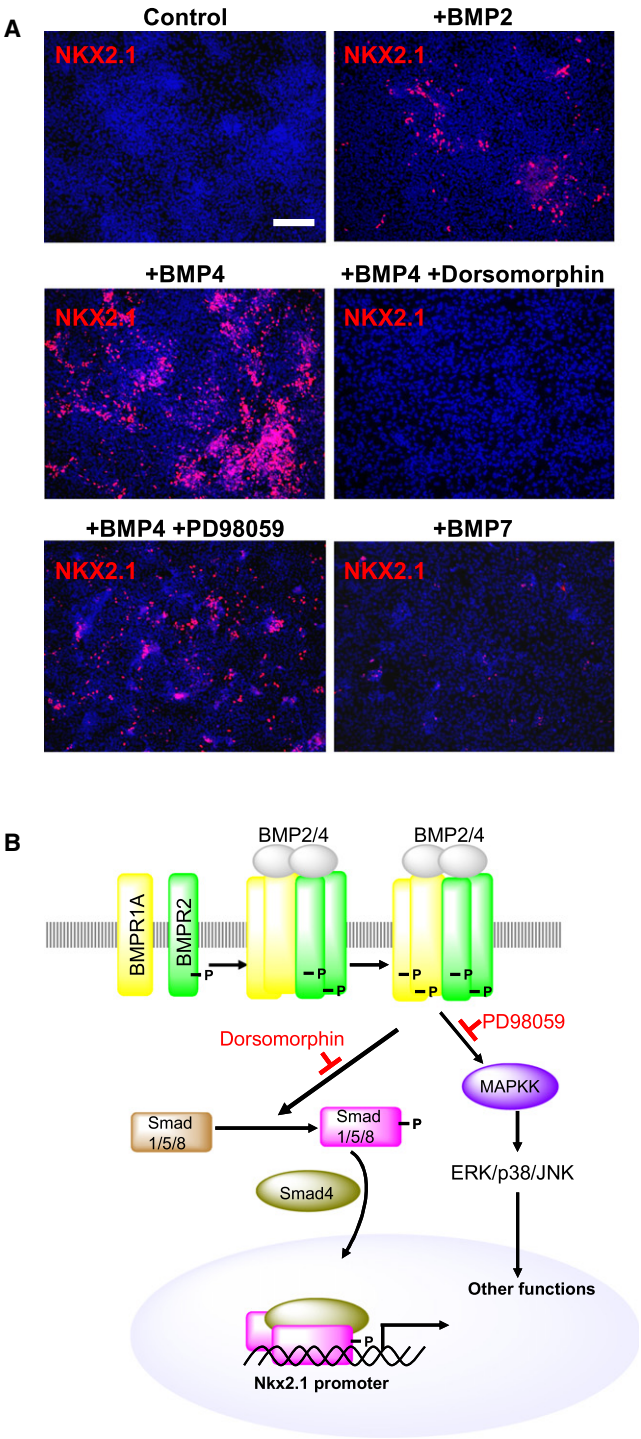

Figure 4. Smad-Dependent BMP Signaling Is Required for Lung Differentiation

(A) NKX2.1 induction with 20 ng/ml FGF2 and 5 nM GSK3iXV only (control) or with additional BMP4 (20 ng/ml), BMP2 (20 ng/ml), BMP7 (20 ng/ml), BMP4 (20 ng/ml) + 10 μM Dorsomorphin, or BMP4 (20 ng/ml) + 1 μM PD98059. Scale bar, 100 μm.

(B) BMP signaling through SMAD-dependent pathways is required for lung Nkx2.1+ differentiation. In contrast, signaling through the MAP kinase pathway is not required for *Nkx2.1* expression. Dorsomorphin inhibits BMP signaling through the SMAD pathway while PD98059 inhibits MAPK signaling.

The Combination of BMP7 and FGF7 Signaling, as well as WNT and MAPKK/ERK Inhibition, Generates Proximal Airway Progenitors

As we demonstrated above, most ESC-derived Nkx2.1+ cells at day 9 were immature lung endoderm cells. We therefore continued to differentiate these cells in order to produce more mature Nkx2.1+Sox2+ embryonic airway progenitors. We selectively applied signaling factors to generate airway stalk progenitors from immature lung Nkx2.1+ cells (Figures 5A and 5B). Multipotent Nkx2.1+Sox9+ tip progenitors replicate at the lung bud tip and their progeny are laid down during the pseudoglandular phase of branching morphogenesis (E11 to E16.5) to constitute the primitive airway tree and differentiate into Nkx2.1+Sox2+ airway progenitors. BMP4 is expressed distally and BMP7 is expressed around the airway, and distal FGF2 and FGF10 are replaced by proximal FGF7 (Weaver et al., 1999; Bellusci et al., 1996; Lebeche et al., 1999; Powell et al., 1998; Morrisey and Hogan, 2010), while canonical WNT signaling is inhibited in the proximal stalk progenitors and present in the distal tip (Shu et al., 2005; Okubo and Hogan, 2004). Similarly, airway stalk cells are exposed to inhibitory Noggin while the uncommitted tip cells are exposed to BMP4 (Weaver et al., 1999; Que et al., 2006). Retinoic acid (RA) concentration is relatively higher in the stalk region than at the tips (Malpel et al., 2000). We therefore switched cells at day 9 to a "proximal induction" medium prepared with RA-supplemented B27, BMP7, FGF7, IWR-1 (WNT antagonist), and Noggin (Figure 5C, left panel). After 2–3 days, we observed an increase in Nkx2.1+Sox2+ airway progenitor cells. The proportion was ~10% of the total number of Nkx2.1+ cells, as compared to 1%–2% before treatment. In separate experiments in which individual growth factors were removed, we found that WNT antagonism has the most pronounced effect on Nkx2.1+Sox2+ cell production. Addition of Dorsomorphin (BMP antagonist) to replace Noggin at this stage had little effect on the number of Nkx2.1+Sox2+ cells. Interestingly, the small molecule PD98059 (a MAPKK/ERK inhibitor) enhanced generation of Nkx2.1+Sox2+ airway progenitor cells to up to 18% of the total number of Nkx2.1+ cells (Figure 5C, right panel). This suggests that airway progenitors may be formed after inhibition of a MAPKK/ERK-related pathway. Most notably, we started to detect a small fraction of Nkx2.1+p63+ cells (about 1%–4% of the total number of Nkx2.1+ cells) at day 11–12 (Figure 5D). An increase in the duration of culture in the proximal induction medium from 2 to 5 or more days resulted in higher proportions of Nkx2.1+Sox2+ and Nkx2.1+p63+ cells (data not shown). Although the production of Nkx2.1+Sox2+ and Nkx2.1+p63+ cells still needs to be optimized, our results demonstrate that ESC-derived Nkx2.1+ cells can be differentiated into proximal airway progenitors and conducting airway basal cells.

ESC-Derived Nkx2.1+ Cell Populations Can Differentiate into Mature Airway Epithelium When Transplanted In Vivo

Nkx2.1+ lung progenitor cells derived from pluripotent stem cells must possess the capacity to generate functional respiratory epithelium to be useful. Therefore, we tested our mouse ESC-derived Nkx2.1+ progenitors for their capacity to form mature respiratory epithelium by subcutaneous engraftment (Figure 6).

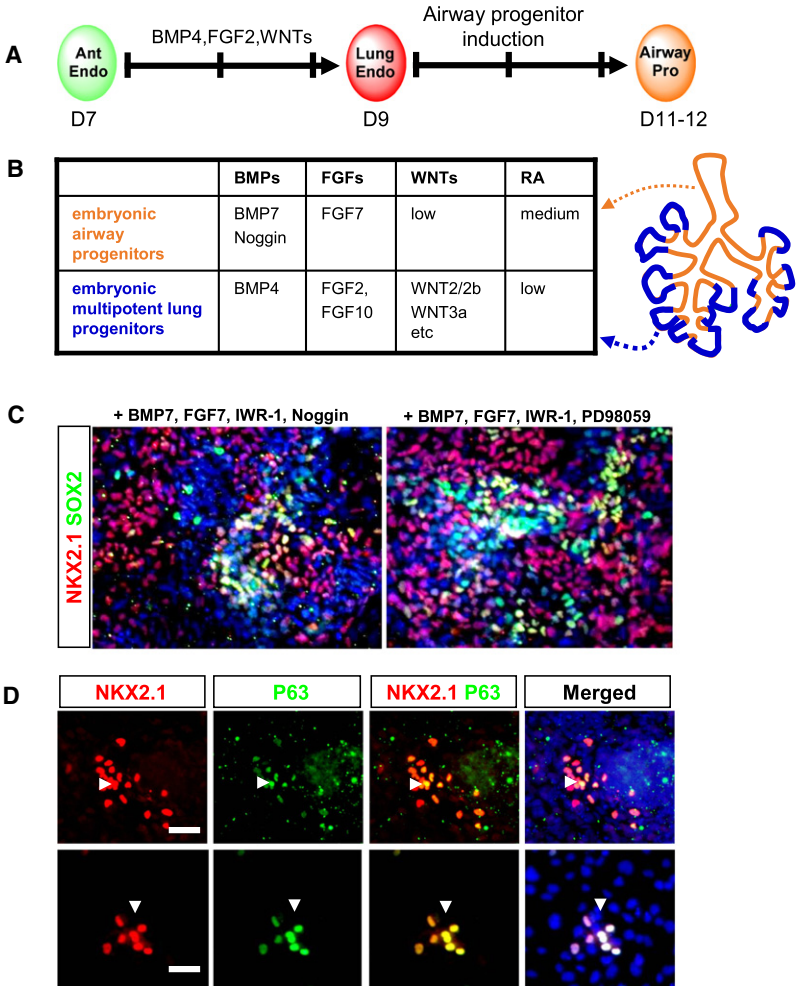

Figure 5. Generation of Embryonic Airway Progenitors from Multipotent Lung Endoderm Cells

(A) Schematic strategy and time line to generate embryonic airway progenitors from multipotent lung endoderm cells.

(B) Summary of signaling switches that are distinct in the proximal airway and the distal lung bud tip during the pseudoglandular stage of lung development.

(C) Left panel: NKX2.1 and SOX2 staining after treatment of Nkx2.1+ lung endoderm cells at D9 with medium containing RA-supplemented B27, 20 ng/ml BMP7, 20 ng/ml FGF7, 100 nM IWR-1 (WNT antagonist), and 100 ng/ml Noggin for 2 days. Right panel: NKX2.1 and SOX2 staining after treatment of Nkx2.1+ lung endoderm cells at D9 with medium containing RA-supplemented B27, 20 ng/ml BMP7, 20 ng/ml FGF7, 100 nM IWR-1 (WNT antagonist), and 1 μM PD98059 for 2 days. Scale bar, 50 μm.

(D) Immunofluorescence staining showing a subpopulation of Nkx2.1+ cells positive for P63 (closed arrows). Scale bar, 25 μm.

Because we cannot separate committed Nkx2.1+Sox2+ airway progenitor cells from other cells, our assay evaluated the ability of Nkx2.1+ cells to differentiate within a mixed cell population. 20,000–50,000 cells were suspended in 50% Matrigel and injected under the skin of immunodeficient mice. Twenty to thirty days after injection, engrafted tissues were excised for examination. We observed that many epithelial spheres formed within grafts and that some of these spheres contained Nkx2.1-expressing cells. In some Nkx2.1+ spheres, we detected markers of mature airway epithelial cells (Figure 6), including Sox2+ proximal airway epithelial cells (Figure 6B), p63+ basal stem cells, CC10+ Clara cells, FoxJ1+ ciliated cells, and Muc5ac+ mucin-secreting cells (Figures 6C and 6D). Triple immunofluorescence staining with confocal imaging demonstrated spheres that contain more than one marker of mature airway epithelium. Such mature airway epithelial markers have never been detected in ESC-derived teratomas. Previously published basal stem cell differentiation using a 3D sphere-forming assay produced ciliated and basal cells, but not Clara cells (Rock et al., 2009). We did not detect any type I and type II pneumocyte markers such as PRO-SPC, PRO-SPA, and AQUAPORIN5 despite having distal lung multipotent cells (Nkx2.1+Sox9+ and Nkx2.1+FoxP2+) in the initial cell mixture. Overall, we concluded that ESC-derived Nkx2.1+ cell-containing populations are capable of airway epithelial cell differentiation.

An Efficient and Reproducible Stepwise Approach to Generate NKX2.1+ Lung Cells from Human CF iPSCs

Next, we examined whether a similar stepwise differentiation approach could be used to generate lung airway progenitors from CF disease-specific human iPSCs (Figure 7A). All differentiation steps were performed in xeno-free conditions. Furthermore, two of the CF iPSC lines were generated using modified RNAs (RiPSC) rather than virally encoded reprogramming factors (Warren et al., 2010) and thus were genetically unmodified, another advantage for possible future clinical use. CF iPSCs were maintained on Geltrex-coated plates in complete mTeSR1 medium. High yields of DE were obtained after treatment for 3–4 days in RPMI-1640 medium in the presence of Activin (100 ng/ml) and PI3 kinase inhibitor LY294002 (5 μM). More than 85%–90% of cells coexpressed the transcription factors SOX17 and FOXA2 at day 4, demonstrating very efficient production of DE from a RiPSC line that is compound heterozygous for *CFTR* mutant alleles ΔF508 and G551D (Figure 7B). This protocol was also successfully applied to other human pluripotent cells including three CF iPSC lines homozygous for the ΔF508 allele, a wild-type human BJ RiPSC line (Warren et al., 2010), and the HUES-3 and HUES-9 human ESC lines (data not shown).

By using anteriorization conditions similar to those used by Green et al., we were able to induce SOX2 expression in DE cells with efficiencies of up to 50%–60% after 4 days of treatment with A-83-01 (a TGFβ antagonist; Figure 7C). We found that Noggin (a BMP4 antagonist) was actually not necessary for this anteriorization. Similar combinations of growth factors and agonists (BMP4, FGF2, and GSK3iXV) identified in our studies on mouse ESCs could be used to generate Nkx2.1+ cells with efficiencies of 10%–30% (Figure 7D). These Nkx2.1+ cells were negative for

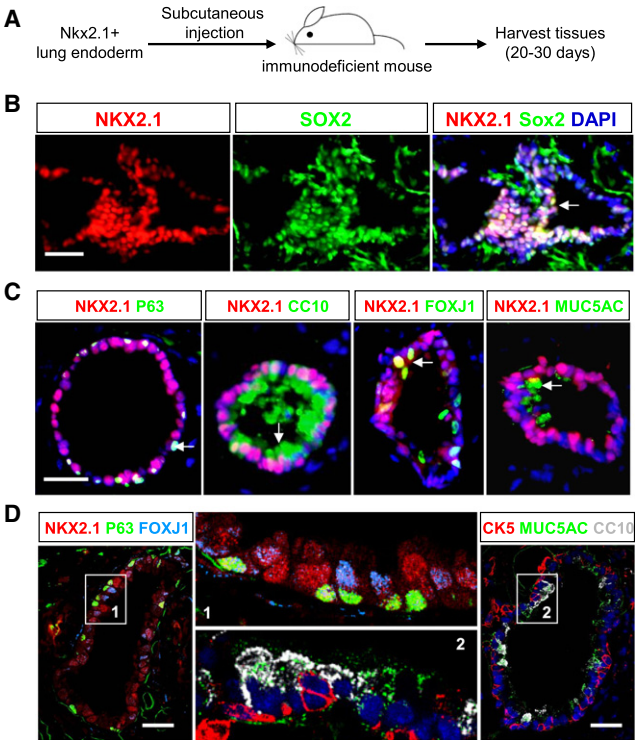

Figure 6. Differentiation of Airway Epithelium from Mouse-ESC-Derived Lung Endoderm upon Subcutaneous Engraftment

(A) Schematic strategy and time line to differentiate ESC-derived embryonic airway progenitors.

(B) Immunofluorescence staining showing that some Nkx2.1+ cells are positive for SOX2. Scale bar, 100 μm.

(C) Immunofluorescence staining showing differentiation of ESC-derived Nkx2.1+ cells into p63+ airway basal stem cells, CC10+ Clara cells, FoxJ1+ ciliated cells, and Muc5ac+ goblet cells. The arrow points to a representative positive cell for each category. Scale bar, 100 μm.

(D) Confocal imaging showing differentiation of various airway epithelial cells. Scale bar, 100 μm.

TUJ1 and PAX8 (Figure 7D), demonstrating that they were not of neuronal or thyroid identity. In addition, subpopulations of these Nkx2.1+ cells were also positive for SOX2 and SOX9 (Figure 7D). These markers suggest the presence of both committed airway progenitors (Nkx2.1+Sox2.1 cells) and multipotent embryonic lung progenitors (Nkx2.1+Sox9+ cells).

We also quantified the expression of various anterior cell fate genes by qPCR (Figure S4) and observed very similar gene expression patterns to those seen in mouse ESC differentiation. *SOX2* was downregulated after differentiation into DE and then increased as expected after anteriorization. We again observed dramatic upregulation of *NKX2.1*, *SOX9*, and *FOXP2* expression (20–30 fold) in anteriorized endoderm cells after FGF2/BMP4/WNT induction. The expression of other anterior cell fate genes including *PAX8* (thyroid endoderm), *PAX9* (pharyngeal endoderm), and *TBX1* (pharyngeal endoderm anterior to lung/esophagus) was only modestly upregulated without any expression of *FOXN1* (thymus endoderm) (Figure S5). In aggregate, the differentiation spectrum of the endoderm was remarkably similar in the mouse and human platforms.

Finally, human RiPSC-derived Nkx2.1+ mixed cell populations were subcutaneously engrafted (Figure 7E). Many spheres formed in engrafted tissues after 30 days under the skin of immunodeficient recipient mice. In Nkx2.1+ spheres, some of the Nkx2.1+ cells coexpressed p63, suggesting that these Nkx2.1+ cells had matured into airway basal stem cells (Figure 7E). Further differentiation into ciliated cells, Clara cells, and mucin-secreting goblet cells was not detected, indicating that further optimization of differentiation conditions is required.

DISCUSSION

We report a stepwise developmentally guided strategy to differentiate murine pluripotent stem cells into lung multipotent progenitors and airway progenitors that produced respiratory epithelium when engrafted subcutaneously into a mouse. We then adapted our strategy to produce disease-specific lung progenitor cells from human CF iPSCs and other human pluripotent stem cell lines, thus creating a platform for dissecting human lung disease.

Additionally, we show that pluripotent stem cell systems can be used as a discovery tool to investigate steps in lung development. We were able to independently confirm recent mouse developmental genetics findings demonstrating that BMP4 is essential for lung specification, as well as similar studies that show that canonical WNT signaling is necessary for lung bud specification (Domyan et al., 2011; Goss et al., 2009). We also demonstrate that FGF signaling in addition to BMP and WNT signaling is required in the current culture system for NKX2.1 induction, an observation that has proven difficult to define in murine genetic systems due to the presence of multiple FGFs in the vicinity of the foregut lung anlage. Mechanistic dissection of the BMP4 signaling effect also revealed an observation that BMP4 signaling occurs through a Smad-dependent pathway and that pharmacologic Smad modulation enhances Nkx2.1+ lung cell differentiation. We have also shown that the carefully timed staged antagonism or agonism of the same pathway is essential to drive optimal differentiation. The premature addition of WNT signals that are later necessary for Nkx2.1+ lung cell induction at the endoderm stage, for example, regionalizes endoderm to a hindgut intestinal epithelium and prevents the differentiation of Nkx2.1+ cells (Spence et al., 2011; Cao et al., 2011; Sherwood et al., 2011). Thus, not only combinations of signaling cascades, but also their precise timing, are essential to recapitulate in vivo differentiation.

Although we report differentiation of Nkx2.1+Sox2+ proximal airway progenitors and Nkx2.1+p63+ double-positive airway stem cells derived from both human and mouse pluripotent stem cells, the proportions of Nkx2.1+ lung and airway progenitors are low. This might reflect an intrinsic bias in the differentiation of our iPSCs. It is also possible that other pathways cooperate with FGF, BMP, and WNT signaling cascades to effect Nkx2.1+ endoderm differentiation or, conversely, that other pathways need to be inhibited. Zaret and colleagues have suggested that the anterior gut contains an epigenetic prepattern that regulates the ability of gut endoderm to differentiate into a particular tissue despite the presence of the correct growth factors (Zaret et al., 2008). Perhaps many of the iPSC-derived foregut endoderm cells do not possess the epigenetic prepattern

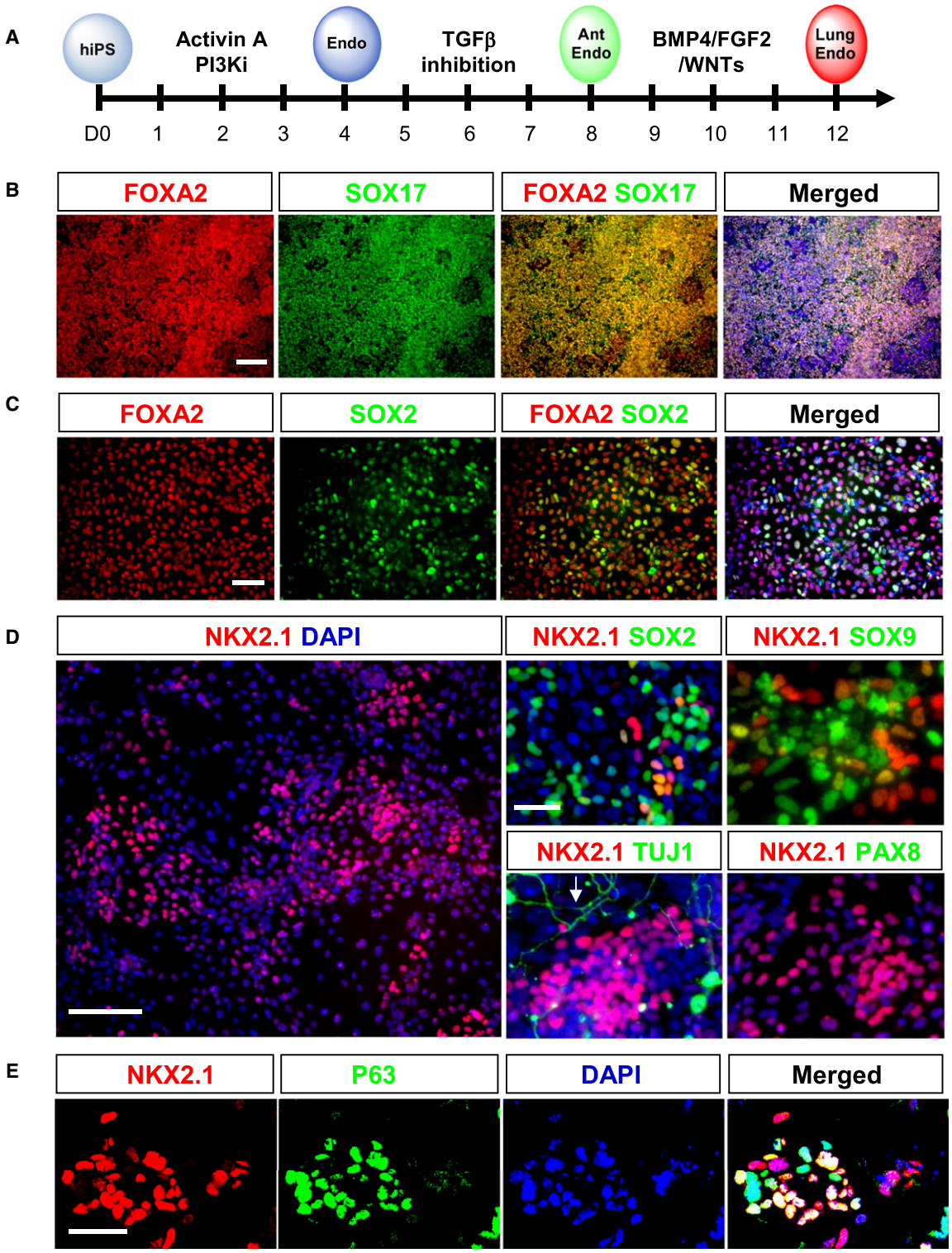

Figure 7. Stepwise Differentiation of Nkx2.1+ Lung Progenitors from Human iPSCs

(A) Schematic strategy and time line to generate Nkx2.1+ lung multipotent progenitors from human iPSCs.

(B) High yield of definitive endoderm from CF1 RiPSCs was obtained after treatment for 4 days in RPMI-1640 medium in the presence of 2% B27 supplement, Activin A (100 ng/ml), and 5 μM PI3 Kinase inhibitor LY294002 with more than 90% of cells coexpressing transcription factors SOX17 and FOXA2. Scale bar, 200 μm.

(C) Anteriorization of endoderm into foregut endoderm cells with SOX2 expression in Foxa2+ cells derived from CF1 RiPSCs after 4 days of treatment with 500 nM A-83-01 (TGFβ antagonist) and 100 ng/ml Noggin (BMP4 antagonist). Scale bar, 100 μm.

that would allow them to differentiate into Nkx2.1 cells. Additionally, it must be determined whether Nkx2.1+ progenitor cells expanded in culture undergo modifications that permit the expression of thyroid or neuronal genes. It will be important to investigate each of these possibilities so that we can rationally increase the efficiency of the differentiation protocols described herein by overcoming the relevant mechanistic hurdles. Ultimately, we will need protocols that will be effective for any human iPSC line and reagents to be able to sort pure populations of human cells in the absence of genetic reporters or selectable drug resistance genes. Our strategy can then in principle be applied to any human lung disorder.

Finally, conditions must be found to affect the maturation of iPSC-derived lung epithelium ex vivo. To study an airways disease like CF and to screen for small molecule therapeutics using iPSC-derived cells, we will require an Nkx2.1+ epithelium that contains all of the appropriate human cellular constituents. That same epithelium must display functional coordinated ciliary beating, epithelial secretory function (including regulated CFTR-mediated chloride ion transport and mucus secretion), and an airway stem cell-driven capacity for epithelial regeneration.

EXPERIMENTAL PROCEDURES

Mice and Human Cell Lines

NOD-SCID IL2Rgamma null (NOD/SCID*Il2rg*$^{-/-}$) immunodeficient mice were purchased from Jackson Laboratory. Animal procedures were performed in accordance with Massachusetts General Hospital (MGH) and national guidelines and regulations and were approved by the Institutional Animal Care and Use Committee (IACUC) for MGH. The use of human CF induced-pluripotent cell lines and embryonic cell lines (HUES-3 and HUES-9) was reviewed and approved by the Embryonic Stem Cell Research Oversight committee (ESCRO) and IRB at MGH.

Mouse Endoderm Anteriorization and Nkx2.1 Cell Differentiation

Mouse DE was generated as described in Supplemental Experimental Procedures. To anteriorize endoderm, on and after day 5, the cells were split and reseeded on to the plates precoated with 804G-conditioned medium and fed with D0 medium + 0.5–1 μM A8301 (CalBiochem, 616454) for 2 days. Then the medium was rinsed with D0 medium two times and switched to D0 medium supplemented with 50 ng/ml BMP4, 100 ng/ml FGF2 (GIBCO, PHG0026), and 5–10 nM GSK3iXV for another 2–3 days. To generate Nkx2.1+Sox2+ proximal progenitor cells, the cells were rinsed with D0 medium two times and switched to D0 medium containing RA-supplemented B27, 50 ng/ml BMP7, 50 ng/ml FGF7, 100 nM IWR-1, and 1–2 μM PD98059 for 2 days or longer.

Human iPSC Culture and Differentiation

Human iPSCs were maintained on Geltrex-coated plates in complete mTeSR1 medium (Stemcell). High yields of DE progenitors were obtained after treatment for 3–4 days in RPMI-1640 medium in the presence of 2% B27 supplement minus vitamin A (GIBCO, 12587-010), Activin A (Peprotech, 100 ng/ml) and PI3 Kinase inhibitor LY294002 (5 μM). To generate foregut endoderm cells, DE was treated for 4 days with RPMI-1640 medium containing 2% B27 and 500 nM A-83-01 (TGFβ antagonist) with or without Noggin (BMP4 antagonist, 100 ng/ml) or Dorsomorphin (2–5 μM). After that, the cells were exposed for 4 days or longer to RPMI-1640 medium containing 2% B27, 50 ng/ml BMP4, 100 ng/ml FGF2, and 5 nM GSK3iXV for NKX2.1 induction from endoderm cells.

Immunofluorescence

At each differentiation step, the cells were fixed with fresh paraformaldehyde (4%) for 15 min at room temperature, rinsed in PBS, washed with PBS + 0.2% Triton X-100, and incubated with the primary antibodies at 4°C overnight (>16 hr) diluted in PBS + 1% BSA. Following incubation, the cells were rinsed four times in PBS + 0.2% Triton X-100, and incubated with secondary antibodies at room temperature for 2 hr. The images were visualized using an Olympus IX71 inverted fluorescence microscope or a Nikon A1 Confocal Laser microscope. The primary antibodies used are summarized in Table S2. The secondary antibodies were purchased from Invitrogen (Alexa Fluor 549 and Alexa Fluor 488). The quantification was performed by counting at least five random fields at 20× magnification and calculating the average and standard deviation.

Embryo Harvest, Section Cutting, and Staining

The embryos or lungs at desired embryonic stages were dissected out and fixed at 4°C for 6 hr or overnight with fresh 4% PFA. Then tissues were rinsed with PBS for 3 min (5 min per time) and incubated in 30% sucrose in PBS at 4°C overnight. The tissues were soaked in OCT for 1 hr and then frozen in OCT for cryosectioning at 7 μm thickness. The slides were stained with the primary and secondary antibodies as described above.

Differentiation of Mouse ESC and Human iPSC-Derived Nkx2.1+ Lung Progenitors after Subcutaneous Engraftment

Anywhere from 2×10^5 to 5×10^5 cells were suspended in 200 μl 1:1 mixture of Growth Factor Reduced Matrigel (BD Biosciences, 354230) and Advanced DMEM and were injected subcutaneously into NOD/SCID*Il2rg*$^{-/-}$ null mice. The tissues were harvested and examined after 20–30 days, fixed overnight in cold 4% paraformaldehyde, rinsed two times with PBS, soaked in 30% sucrose for 2–3 hr, embedded in OCT, and sectioned at 7 μm. The slides were examined for airway epithelial cells based on NKX2.1 expression. The differentiation of ESC-derived Nkx2.1+ cells into basal stem cells was based on expression of P63 and CK5; goblets cells, based on expression of MUC5AC; Clara cells, based on expression of CCSP; and ciliated cells, based on the expression of FOXJ1.

Additional Culture Information

For more information on how to culture these cells, please refer to the Rajagopal Lab website: http://www.massgeneral.org/regenmed/staff/Rajagopallab. We intend to deposit the reported cells in the Harvard Stem Cell Institute iPS Cell Core Facility (please see http://www.hsci.harvard.edu/ipscore/node/3).

SUPPLEMENTAL INFORMATION

Supplemental Information includes four figures, two tables, and Supplemental Experimental Procedures and can be found with this article online at doi:10.1016/j.stem.2012.01.018.

ACKNOWLEDGMENTS

The work in this manuscript was supported by a Harvard Stem Cell Institute Seed Grant and an NIH-NHLBI Early Career Research New Faculty (P30) award to J.R. We thank Drs. William Anderson and Darrell Kotton for reading this manuscript and for their critical comments. We also wish to extend our thanks to all of the members of the Rajagopal Laboratory for their reading of the text, their constructive criticisms and comments, and valuable discussion and support.

Received: August 11, 2011
Revised: December 15, 2011
Accepted: January 19, 2012
Published: April 5, 2012

(D) Left panel: NKX2.1 staining after anteriorization to foregut cells at D8 with serum-free medium containing 20 ng/ml BMP4, 20 ng/ml FGF2, and 5 nM GSK3iXV for 4 days. Scale bar, 100 μm. Right panel: costaining of Nkx2.1-positive cells with SOX2, SOX9, TUJ1 (arrows), and PAX8 demonstrated a lack of thyroid and neuronal differentiation and the presence of multipotent distal tip progenitors and Nkx2.1+/Sox2+ airway progenitors. Scale bar, 50 μm.
(E). Confocal image after immunofluorescence staining showing that some Nkx2.1+ spheres contain basal cells positive for p63. Scale bar, 40 μm.

REFERENCES

Accurso, F.J., Rowe, S.M., Clancy, J.P., Boyle, M.P., Dunitz, J.M., Durie, P.R., Sagel, S.D., Hornick, D.B., Konstan, M.W., Donaldson, S.H., et al. (2010). Effect of VX-770 in persons with cystic fibrosis and the G551D-CFTR mutation. N. Engl. J. Med. *363*, 1991–2003.

Ameri, J., Ståhlberg, A., Pedersen, J., Johansson, J.K., Johannesson, M.M., Artner, I., and Semb, H. (2010). FGF2 specifies hESC-derived definitive endoderm into foregut/midgut cell lineages in a concentration-dependent manner. Stem Cells *28*, 45–56.

Aubin, J., Davy, A., and Soriano, P. (2004). In vivo convergence of BMP and MAPK signaling pathways: impact of differential Smad1 phosphorylation on development and homeostasis. Genes Dev. *18*, 1482–1494.

Bellusci, S., Henderson, R., Winnier, G., Oikawa, T., and Hogan, B.L. (1996). Evidence from normal expression and targeted misexpression that bone morphogenetic protein (Bmp-4) plays a role in mouse embryonic lung morphogenesis. Development *122*, 1693–1702.

Cao, L., Gibson, J.D., Miyamoto, S., Sail, V., Verma, R., Rosenberg, D.W., Nelson, C.E., and Giardina, C. (2011). Intestinal lineage commitment of embryonic stem cells. Differentiation *81*, 1–10.

Chen, D., Zhao, M., and Mundy, G.R. (2004). Bone morphogenetic proteins. Growth Factors *22*, 233–241.

Clarke, L.L., Grubb, B.R., Gabriel, S.E., Smithies, O., Koller, B.H., and Boucher, R.C. (1992). Defective epithelial chloride transport in a gene-targeted mouse model of cystic fibrosis. Science *257*, 1125–1128.

Coraux, C., Nawrocki-Raby, B., Hinnrasky, J., Kileztky, C., Gaillard, D., Dani, C., and Puchelle, E. (2005). Embryonic stem cells generate airway epithelial tissue. Am. J. Respir. Cell Mol. Biol. *32*, 87–92.

Cutting, G.R. (2005). Modifier genetics: cystic fibrosis. Annu. Rev. Genomics Hum. Genet. *6*, 237–260.

Domyan, E.T., Ferretti, E., Throckmorton, K., Mishina, Y., Nicolis, S.K., and Sun, X. (2011). Signaling through BMP receptors promotes respiratory identity in the foregut via repression of Sox2. Development *138*, 971–981.

Drumm, M.L., Konstan, M.W., Schluchter, M.D., Handler, A., Pace, R., Zou, F., Zariwala, M., Fargo, D., Xu, A., Dunn, J.M., et al; Gene Modifier Study Group. (2005). Genetic modifiers of lung disease in cystic fibrosis. N. Engl. J. Med. *353*, 1443–1453.

Goss, A.M., Tian, Y., Tsukiyama, T., Cohen, E.D., Zhou, D., Lu, M.M., Yamaguchi, T.P., and Morrisey, E.E. (2009). Wnt2/2b and beta-catenin signaling are necessary and sufficient to specify lung progenitors in the foregut. Dev. Cell *17*, 290–298.

Green, M.D., Chen, A., Nostro, M.C., d'Souza, S.L., Schaniel, C., Lemischka, I.R., Gouon-Evans, V., Keller, G., and Snoeck, H.W. (2011). Generation of anterior foregut endoderm from human embryonic and induced pluripotent stem cells. Nat. Biotechnol. *29*, 267–272.

Guilbault, C., Saeed, Z., Downey, G.P., and Radzioch, D. (2007). Cystic fibrosis mouse models. Am. J. Respir. Cell Mol. Biol. *36*, 1–7.

Haston, C.K., and Hudson, T.J. (2005). Finding genetic modifiers of cystic fibrosis. N. Engl. J. Med. *353*, 1509–1511.

Kerem, B., Rommens, J.M., Buchanan, J.A., Markiewicz, D., Cox, T.K., Chakravarti, A., Buchwald, M., and Tsui, L.C. (1989). Identification of the cystic fibrosis gene: genetic analysis. Science *245*, 1073–1080.

Kerem, E., Corey, M., Kerem, B.S., Rommens, J., Markiewicz, D., Levison, H., Tsui, L.C., and Durie, P. (1990). The relation between genotype and phenotype in cystic fibrosis—analysis of the most common mutation (delta F508). N. Engl. J. Med. *323*, 1517–1522.

Kerem, E., Reisman, J., Corey, M., Canny, G.J., and Levison, H. (1992). Prediction of mortality in patients with cystic fibrosis. N. Engl. J. Med. *326*, 1187–1191.

Knowles, M.R. (2006). Gene modifiers of lung disease. Curr. Opin. Pulm. Med. *12*, 416–421.

Kozawa, O., Hatakeyama, D., and Uematsu, T. (2002). Divergent regulation by p44/p42 MAP kinase and p38 MAP kinase of bone morphogenetic protein-4-stimulated osteocalcin synthesis in osteoblasts. J. Cell. Biochem. *84*, 583–589.

Lazzaro, D., Price, M., de Felice, M., and Di Lauro, R. (1991). The transcription factor TTF-1 is expressed at the onset of thyroid and lung morphogenesis and in restricted regions of the foetal brain. Development *113*, 1093–1104.

Lebeche, D., Malpel, S., and Cardoso, W.V. (1999). Fibroblast growth factor interactions in the developing lung. Mech. Dev. *86*, 125–136.

Malpel, S., Mendelsohn, C., and Cardoso, W.V. (2000). Regulation of retinoic acid signaling during lung morphogenesis. Development *127*, 3057–3067.

Minoo, P., Su, G., Drum, H., Bringas, P., and Kimura, S. (1999). Defects in tracheoesophageal and lung morphogenesis in Nkx2.1(-/-) mouse embryos. Dev. Biol. *209*, 60–71.

Miyazono, K., Kamiya, Y., and Morikawa, M. (2010). Bone morphogenetic protein receptors and signal transduction. J. Biochem. *147*, 35–51.

Morrisey, E.E., and Hogan, B.L. (2010). Preparing for the first breath: genetic and cellular mechanisms in lung development. Dev. Cell *18*, 8–23.

Okubo, T., and Hogan, B.L. (2004). Hyperactive Wnt signaling changes the developmental potential of embryonic lung endoderm. J. Biol. *3*, 11.

Perl, A.K., Kist, R., Shan, Z., Scherer, G., and Whitsett, J.A. (2005). Normal lung development and function after Sox9 inactivation in the respiratory epithelium. Genesis *41*, 23–32.

Powell, P.P., Wang, C.C., Horinouchi, H., Shepherd, K., Jacobson, M., Lipson, M., and Jones, R. (1998). Differential expression of fibroblast growth factor receptors 1 to 4 and ligand genes in late fetal and early postnatal rat lung. Am. J. Respir. Cell Mol. Biol. *19*, 563–572.

Que, J., Choi, M., Ziel, J.W., Klingensmith, J., and Hogan, B.L. (2006). Morphogenesis of the trachea and esophagus: current players and new roles for noggin and Bmps. Differentiation *74*, 422–437.

Que, J., Luo, X., Schwartz, R.J., and Hogan, B.L. (2009). Multiple roles for Sox2 in the developing and adult mouse trachea. Development *136*, 1899–1907.

Rawlins, E.L., Clark, C.P., Xue, Y., and Hogan, B.L. (2009). The Id2+ distal tip lung epithelium contains individual multipotent embryonic progenitor cells. Development *136*, 3741–3745.

Riordan, J.R., Rommens, J.M., Kerem, B., Alon, N., Rozmahel, R., Grzelczak, Z., Zielenski, J., Lok, S., Plavsic, N., Chou, J.L., et al. (1989). Identification of the cystic fibrosis gene: cloning and characterization of complementary DNA. Science *245*, 1066–1073.

Rock, J.R., Onaitis, M.W., Rawlins, E.L., Lu, Y., Clark, C.P., Xue, Y., Randell, S.H., and Hogan, B.L. (2009). Basal cells as stem cells of the mouse trachea and human airway epithelium. Proc. Natl. Acad. Sci. USA *106*, 12771–12775.

Rogers, C.S., Stoltz, D.A., Meyerholz, D.K., Ostedgaard, L.S., Rokhlina, T., Taft, P.J., Rogan, M.P., Pezzulo, A.A., Karp, P.H., Itani, O.A., et al. (2008). Disruption of the CFTR gene produces a model of cystic fibrosis in newborn pigs. Science *321*, 1837–1841.

Roszell, B., Mondrinos, M.J., Seaton, A., Simons, D.M., Koutzaki, S.H., Fong, G.H., Lelkes, P.I., and Finck, C.M. (2009). Efficient derivation of alveolar type II cells from embryonic stem cells for in vivo application. Tissue Eng. Part A *15*, 3351–3365.

Samadikuchaksaraei, A., Cohen, S., Isaac, K., Rippon, H.J., Polak, J.M., Bielby, R.C., and Bishop, A.E. (2006). Derivation of distal airway epithelium from human embryonic stem cells. Tissue Eng. *12*, 867–875.

Serls, A.E., Doherty, S., Parvatiyar, P., Wells, J.M., and Deutsch, G.H. (2005). Different thresholds of fibroblast growth factors pattern the ventral foregut into liver and lung. Development *132*, 35–47.

Sherwood, R.I., Maehr, R., Mazzoni, E.O., and Melton, D.A. (2011). Wnt signaling specifies and patterns intestinal endoderm. Mech. Dev. *128*, 387–400.

Shu, W., Guttentag, S., Wang, Z., Andl, T., Ballard, P., Lu, M.M., Piccolo, S., Birchmeier, W., Whitsett, J.A., Millar, S.E., and Morrisey, E.E. (2005). Wnt/beta-catenin signaling acts upstream of N-myc, BMP4, and FGF signaling to regulate proximal-distal patterning in the lung. Dev. Biol. *283*, 226–239.

Shu, W., Lu, M.M., Zhang, Y., Tucker, P.W., Zhou, D., and Morrisey, E.E. (2007). Foxp2 and Foxp1 cooperatively regulate lung and esophagus development. Development *134*, 1991–2000.

Sieber, C., Kopf, J., Hiepen, C., and Knaus, P. (2009). Recent advances in BMP receptor signaling. Cytokine Growth Factor Rev. *20*, 343–355.

Snouwaert, J.N., Brigman, K.K., Latour, A.M., Malouf, N.N., Boucher, R.C., Smithies, O., and Koller, B.H. (1992). An animal model for cystic fibrosis made by gene targeting. Science *257*, 1083–1088.

Spence, J.R., Mayhew, C.N., Rankin, S.A., Kuhar, M.F., Vallance, J.E., Tolle, K., Hoskins, E.E., Kalinichenko, V.V., Wells, S.I., Zorn, A.M., et al. (2011). Directed differentiation of human pluripotent stem cells into intestinal tissue in vitro. Nature *470*, 105–109.

Stoltz, D.A., Meyerholz, D.K., Pezzulo, A.A., Ramachandran, S., Rogan, M.P., Davis, G.J., Hanfland, R.A., Wohlford-Lenane, C., Dohrn, C.L., Bartlett, J.A., et al. (2010). Cystic fibrosis pigs develop lung disease and exhibit defective bacterial eradication at birth. Sci. Transl. Med. *2*, ra31.

Sun, X., Sui, H., Fisher, J.T., Yan, Z., Liu, X., Cho, H.J., Joo, N.S., Zhang, Y., Zhou, W., Yi, Y., et al. (2010). Disease phenotype of a ferret CFTR-knockout model of cystic fibrosis. J. Clin. Invest. *120*, 3149–3160.

Van Haute, L., De Block, G., Liebaers, I., Sermon, K., and De Rycke, M. (2009). Generation of lung epithelial-like tissue from human embryonic stem cells. Respir. Res. *10*, 105.

Van Vranken, B.E., Romanska, H.M., Polak, J.M., Rippon, H.J., Shannon, J.M., and Bishop, A.E. (2005). Coculture of embryonic stem cells with pulmonary mesenchyme: a microenvironment that promotes differentiation of pulmonary epithelium. Tissue Eng. *11*, 1177–1187.

von Bubnoff, A., and Cho, K.W. (2001). Intracellular BMP signaling regulation in vertebrates: pathway or network? Dev. Biol. *239*, 1–14.

Wang, D., Haviland, D.L., Burns, A.R., Zsigmond, E., and Wetsel, R.A. (2007). A pure population of lung alveolar epithelial type II cells derived from human embryonic stem cells. Proc. Natl. Acad. Sci. USA *104*, 4449–4454.

Warren, L., Manos, P.D., Ahfeldt, T., Loh, Y.H., Li, H., Lau, F., Ebina, W., Mandal, P.K., Smith, Z.D., Meissner, A., et al. (2010). Highly efficient reprogramming to pluripotency and directed differentiation of human cells with synthetic modified mRNA. Cell Stem Cell *7*, 618–630.

Watanabe, K., Kamiya, D., Nishiyama, A., Katayama, T., Nozaki, S., Kawasaki, H., Watanabe, Y., Mizuseki, K., and Sasai, Y. (2005). Directed differentiation of telencephalic precursors from embryonic stem cells. Nat. Neurosci. *8*, 288–296.

Weaver, M., Yingling, J.M., Dunn, N.R., Bellusci, S., and Hogan, B.L. (1999). Bmp signaling regulates proximal-distal differentiation of endoderm in mouse lung development. Development *126*, 4005–4015.

Wells, J.M., and Melton, D.A. (2000). Early mouse endoderm is patterned by soluble factors from adjacent germ layers. Development *127*, 1563–1572.

Wert, S.E., Glasser, S.W., Korfhagen, T.R., and Whitsett, J.A. (1993). Transcriptional elements from the human SP-C gene direct expression in the primordial respiratory epithelium of transgenic mice. Dev. Biol. *156*, 426–443.

Zaret, K.S., Watts, J., Xu, J., Wandzioch, E., Smale, S.T., and Sekiya, T. (2008). Pioneer factors, genetic competence, and inductive signaling: programming liver and pancreas progenitors from the endoderm. Cold Spring Harb. Symp. Quant. Biol. *73*, 119–126.

Zhang, K., Li, L., Huang, C., Shen, C., Tan, F., Xia, C., Liu, P., Rossant, J., and Jing, N. (2010). Distinct functions of BMP4 during different stages of mouse ES cell neural commitment. Development *137*, 2095–2105.